Adoptive cell therapy targeting common p53 neoantigens in human solid cancers

Sanghyun P. Kim[1], Nolan R. Vale[1], Nikolaos Zacharakis[1], Sri Krishna[1], Zhiya Yu[1], Billel Gasmi[2], Jared J. Gartner[1], Sivasish Sindiri[1], Parisa Malekzadeh[1]†, Drew C. Deniger[1]‡, Frank J. Lowery[1], Maria R. Parkhurst[1], Lien T. Ngo[1], Satyajit Ray[1], Yong Li[1], Victoria Hill[1], Maria Florentin[1], Biman C. Paria[1]#, Noam Levin[1], Elizabeth Hedges[1], Agnes Choi[1], Praveen D. Chatani[1], Shoshana Levi[1], Samantha Seitter[1], Yong-Chen Lu[1¶], Zhili Zheng[1], Todd D. Prickett[1], Li Jia[3], Jonathan M. Hernandez[4], Chuong D. Hoang[5], Paul F. Robbins[1], Stephanie L. Goff[1], Richard M. Sherry[1]§, James Yang[1], Steven A. Rosenberg[1*]

*Correspondence to: SAR@NIH.gov

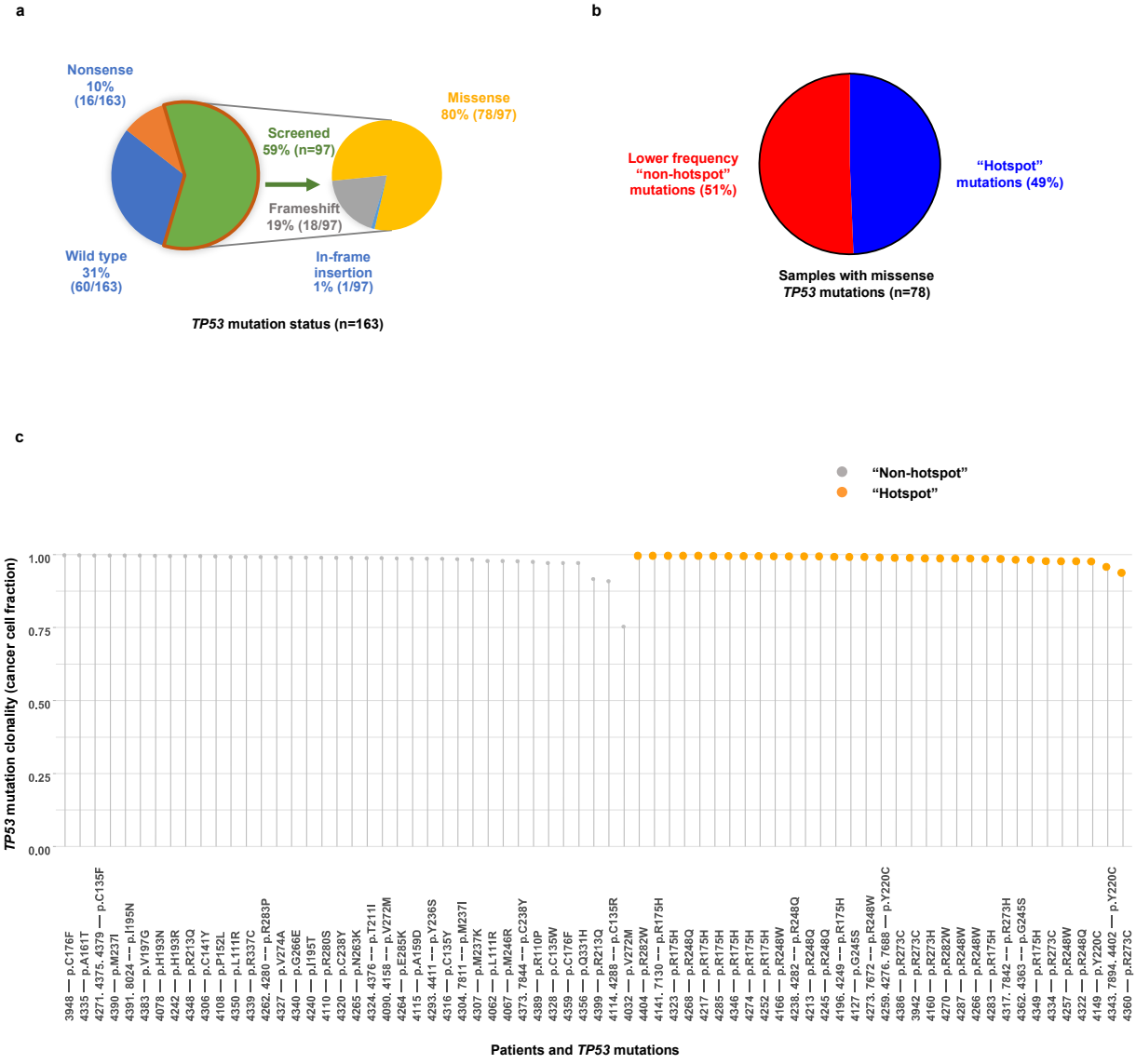
a
Nonsense
10%
(16/163)
Missense
80% (78/97)
Screened
59% (n=97)
Frameshift
19% (18/97)
Wild type
31%
(60/163)
In-frame
insertion
1% (1/97)
TP53 mutation status (n=163)
b
Lower frequency
"non-hotspot"
mutations (51%)
"Hotspot"
mutations (49%)
Samples with missense
TP53 mutations (n=78)
c
"Non-hotspot"
"Hotspot"
TP53 mutation clonality (cancer cell fraction)
1.00
0.75
0.50
0.25
0.00
3948 — p.C176F
4335 — p.A161T
4271. 4375. 4379 — p.C135F
4390 — p.M237I
4391. 8024 — p.I195N
4383 — p.V197G
4078 — p.H193N
4242 — p.H193R
4348 — p.R213Q
4306 — p.C141Y
4108 — p.P152L
4350 — p.L111R
4339 — p.R337C
4262. 4280 — p.R283P
4327 — p.V274A
4340 — p.G266E
4240 — p.I195T
4110 — p.R280S
4320 — p.C238Y
4265 — p.N263K
4324. 4376 — p.T211I
4090. 4158 — p.V272M
4264 — p.E285K
4115 — p.A159D
4293. 4411 — p.Y236S
4316 — p.C135Y
4304. 7811 — p.M237I
4307 — p.M237K
4062 — p.L111R
4067 — p.M246R
4373. 7844 — p.C238Y
4389 — p.R110P
4328 — p.C135W
4359 — p.C176F
4356 — p.Q331H
4399 — p.R213Q
4114. 4288 — p.C135R
4032 — p.V272M
4404 — p.R282W
4141. 7130 — p.R175H
4323 — p.R175H
4268 — p.R248Q
4217 — p.R175H
4285 — p.R175H
4346 — p.R175H
4274 — p.R175H
4252 — p.R175H
4166 — p.R248W
4238. 4282 — p.R248Q
4213 — p.R248Q
4245 — p.R248Q
4196. 4249 — p.R175H
4127 — p.G245S
4273. 7672 — p.R248W
4259. 4276. 7688 — p.Y220C
4386 — p.R273C
3942 — p.R273C
4160 — p.R273H
4270 — p.R282W
4287 — p.R248W
4266 — p.R248W
4283 — p.R175H
4317. 7842 — p.R273H
4362. 4363 — p.G245S
4349 — p.R175H
4334 — p.R273C
4257 — p.R248W
4322 — p.R248Q
4149 — p.Y220C
4343. 7894. 4402 — p.Y220C
4360 — p.R273C
Patients and TP53 mutations

Extended Data Fig. 1. Characteristics of *TP53* mutations in the Surgery Branch cohort. a, Pie chart showing the frequencies of somatic *TP53* mutations within the Surgery Branch patient cohort (n=163). Patients with missense, frameshift and in-frame insertion mutations in *TP53* that consisted 59% of the patients were subjected to the immunogenicity screening for *TP53* mutations. **b,** Pie chart showing the frequencies of “hotspot” and “non-hotspot” *TP53* missense mutations within the Surgery Branch cohort (n=78). **c,** Clonality of “hotspot” and “non-hotspot” *TP53* mutations. The cancer cell fraction values for *TP53* mutations generated from the whole exome sequencing results are plotted. Each dot represents the average clonality for three or more tumor fragments from a single patient.


4316 p53C135Y CD8 TCR-B
DMSO
WT C135 25mer
C135Y 25mer
A*03:01
A*29:02
B*37:01
B*44:03
C*06:02
C*16:01
ALL HLAs

Extended Data Fig. 2. Determination of HLA restriction of CD8 TCR-B isolated from patient 4316. COS7 cells individually transfected with patient 4316's own HLA class I were pulsed with DMSO, wild-type or p53C135Y 25mer peptides and co-cultured with CD8 TCR-B-expressing healthy donor PBLs. ELISpot measurement of IFN-γ secretion is shown.

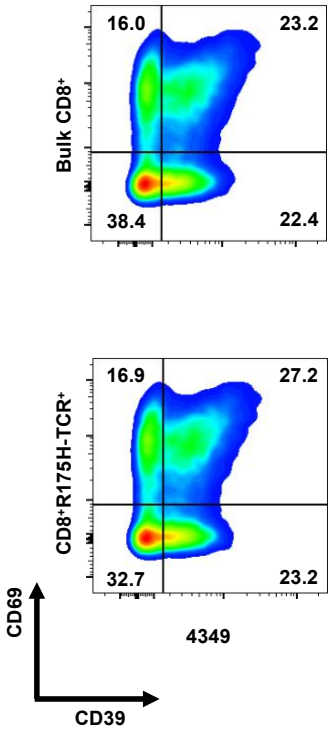
16.0
23.2
Bulk CD8+
38.4
22.4
16.9
27.2
CD8+R175H-TCR+
32.7
23.2
4349
CD69
CD39

Extended Data Fig. 3. Phenotypic analysis of antigen-specific T cells in the infusion products for patients 4349. Phenotypic analysis of antigen-specific (R175H-TCR^{+}) or bulk CD8+ T cells from the infusion products for patient 4349 by flow cytometry. Bulk CD8^{+} T cells (top panel) or CD8^{+}R175H-TCR^{+} cells (bottom panel) were stained for CD39 and CD69.

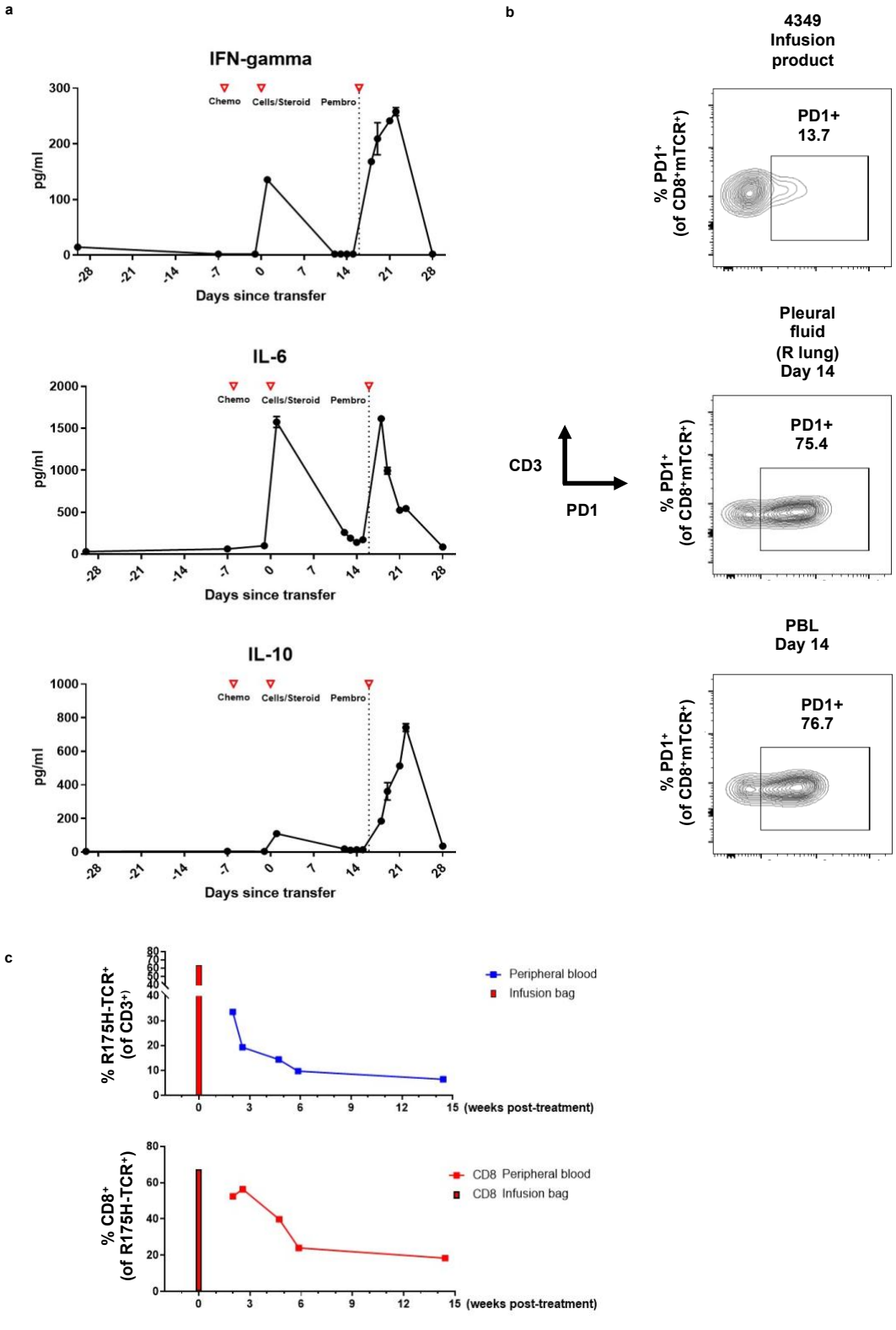
a
IFN-gamma
Chemo
Cells/Steroid
Pembro
pg/ml
Days since transfer
IL-6
IL-10
b
4349
Infusion
product
PD1+
13.7
% PD1+
(of CD8+mTCR+)
Pleural
fluid
(R lung)
Day 14
PD1+
75.4
CD3
PD1
PBL
Day 14
PD1+
76.7
c
% R175H-TCR+
(of CD3+)
Peripheral blood
Infusion bag
(weeks post-treatment)
% CD8+
(of R175H-TCR+)
CD8 Peripheral blood
CD8 Infusion bag

Extended Data Fig. 4. Analysis of T cells and cytokines for patient 4349. a, Serum cytokine levels of IFN-γ (top), IL-6 (middle), and IL-10 (bottom) were measured by a flow cytometry-based LEGENDplex assay. **b,** Flow cytometric analysis of patient 4349's infusion product (top), pleural fluid at day 14 (middle), and PBL at day 14 (bottom) for PD1 expression. **c,** Persistence of R175H-TCR-expressing T cells by flow cytometric detection of R175H-TCR$^+$ T cells (upper panel) and CD8$^+$ T cells of R175H-TCR$^+$ T cells (bottom panel).

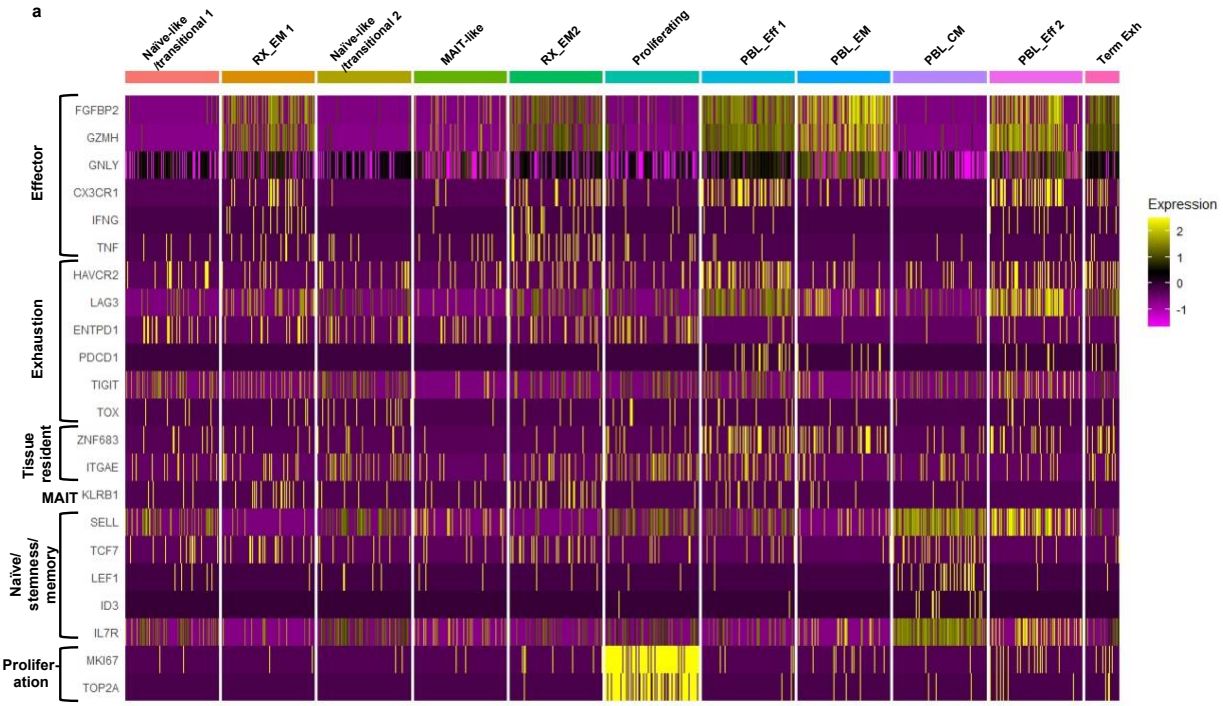
a
Naïve-like /transitional 1
RX_EM 1
Naïve-like /transitional 2
MAIT-like
RX_EM2
Proliferating
PBL_Eff 1
PBL_EM
PBL_CM
PBL_Eff 2
Term Exh
Effector
FGFBP2
GZMH
GNLY
CX3CR1
IFNG
TNF
Exhaustion
HAVCR2
LAG3
ENTPD1
PDCD1
TIGIT
TOX
Tissue resident
ZNF683
ITGAE
MAIT
KLRB1
Naïve/ stemness/ memory
SELL
TCF7
LEF1
ID3
IL7R
Prolifer-ation
MKI67
TOP2A
Expression
2
1
0
-1

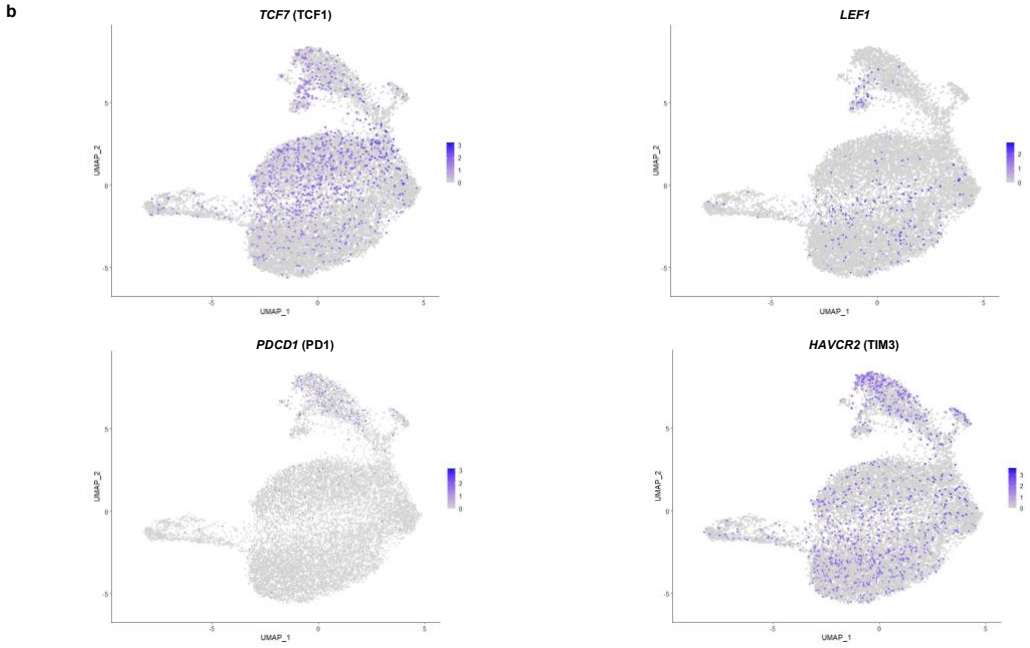
b
TCF7 (TCF1)
LEF1
PDCD1 (PD1)
HAVCR2 (TIM3)
UMAP_1
UMAP_2

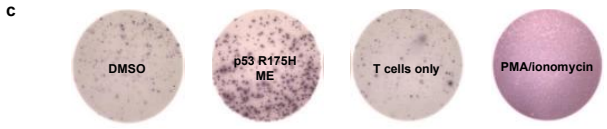
c
DMSO
p53 R175H ME
T cells only
PMA/ionomycin

Extended Data Fig. 5. Analysis of patient 4349's infusion product (RX) and PBL samples post-ACT. a, Heatmap of selected genes across the clusters in Fig. 3F. Expression from each single cell was down sampled to 100 cells per cluster for visibility. **b,** Expression of indicated genes overlaid on the UMAP projection of RX cells and PBL_6w cells. **c,** Functional analysis of PBL sample at 4 months post-ACT. Peripheral blood mononuclear cells were isolated by Ficoll and were subject to co-culture with autologous imDC pulsed with the $p53^{R175H}$ ME or DMSO. T cells only and PMA/ionomycin conditions were included as negative and positive controls, respectively.

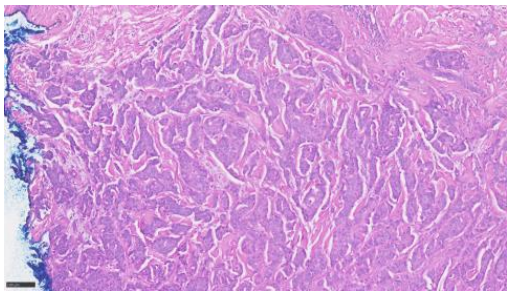

H&E

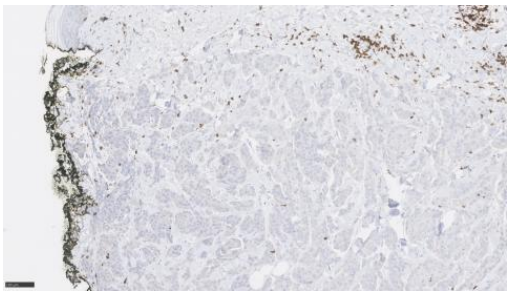

CD3

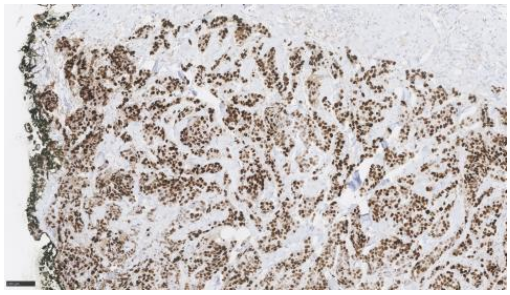

p53

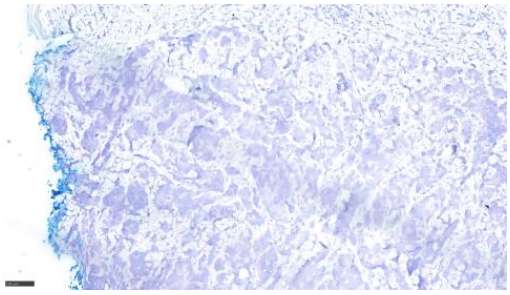

RNAscope (3' UTR of MSGV1)

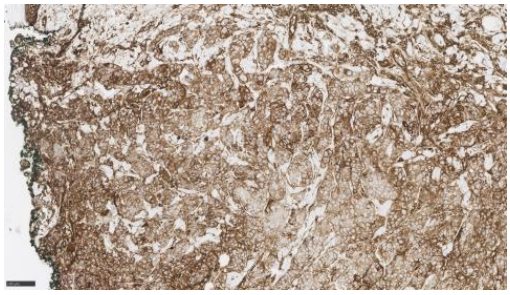

MHC I

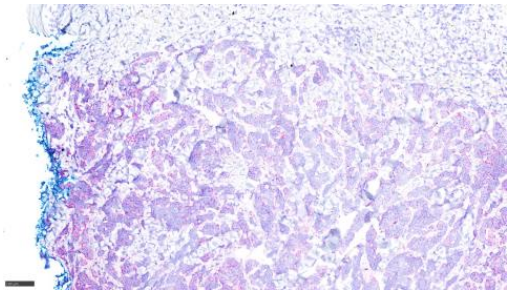

RNAscope [*PP1B* (positive control)]

Extended Data Fig. 6. Analysis of the skin biopsies of patient 4349's progressing lesion. Skin biopsies from patient 4349 at day 209 post-ACT were analyzed by an immunohistochemical and RNAscope analysis. RNAscope against *PP1B* was included as a positive control to ensure the quality of RNA of the specimen. Scale bar, 100 μm.

a

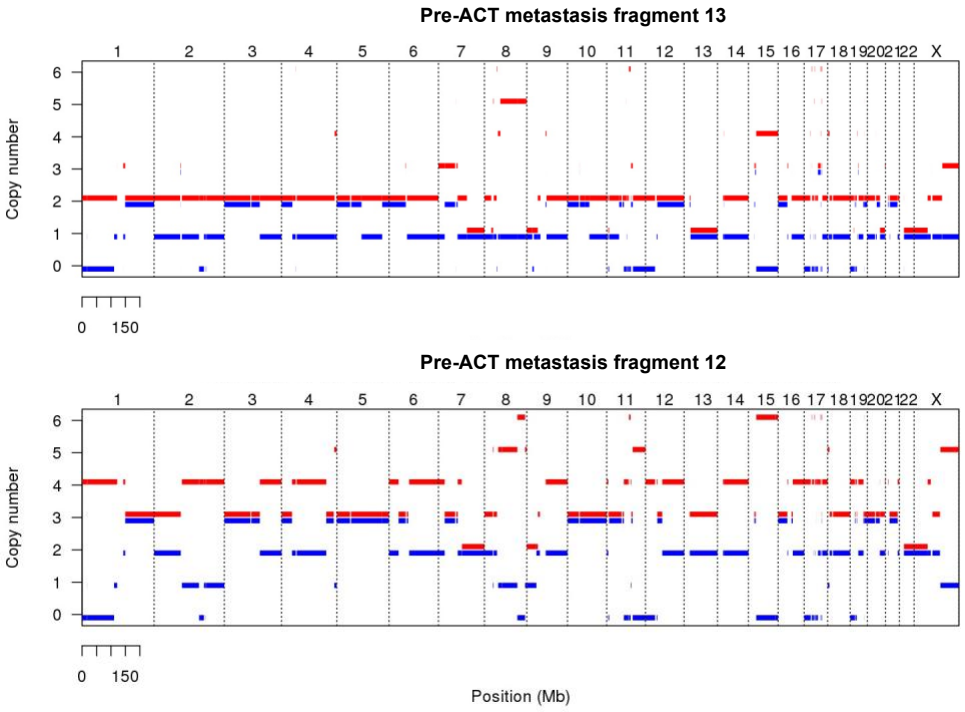
Pre-ACT metastasis fragment 13
Copy number
Pre-ACT metastasis fragment 12
Copy number
Position (Mb)

b

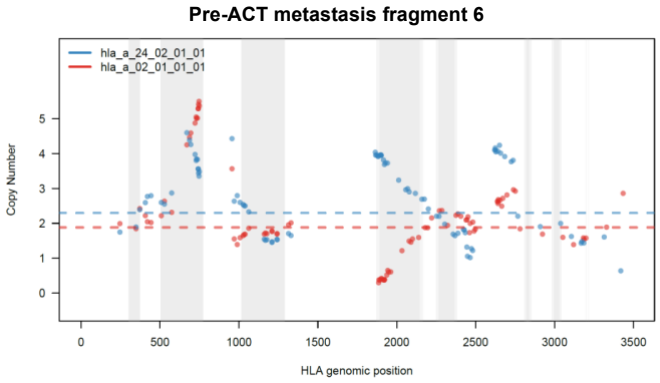
Pre-ACT metastasis fragment 6
hla_a_24_02_01_01
hla_a_02_01_01_01
Copy Number
HLA genomic position

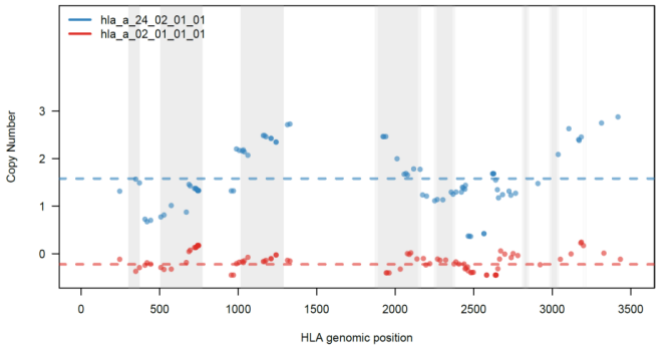
Skin biopsy at recurrence
hla_a_24_02_01_01
hla_a_02_01_01_01
Copy Number
HLA genomic position

Extended Data Fig. 7. Copy number analysis of patient 4349's pre-ACT metastasis sample and the skin biopsy at recurrence by WES. a, Copy number analysis at the chromosome level. **b,** Haplotype specific copy number analysis for the HLA-A locus. Exons are shaded in gray and each dot represents a copy number for a single nucleotide polymorphism corrected for Log R ratio, B allele frequency, tumor purity and tumor ploidy. Dotted lines represent the median allele copy number.

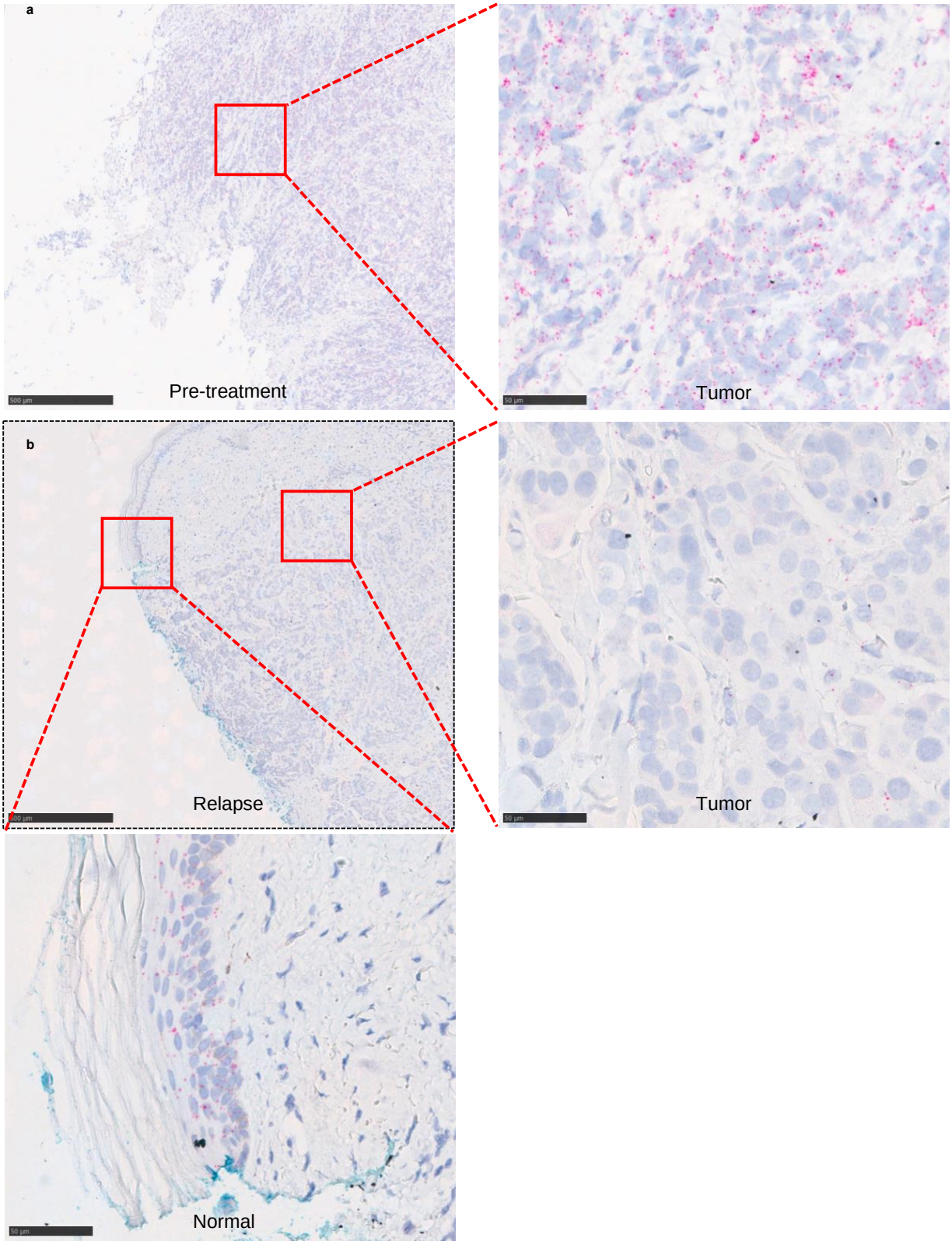
a
Pre-treatment
Tumor
b
Relapse
Tumor
Normal

Extended Data Fig. 8. Detection of HLA-A*02:01 by RNAscope in the pre-ACT and progressing lesion biopsies from patient 4349. Skin biopsies from patient 4349 before the ACT (**a**) and at recurrence at day 209 post-ACT (**b**) were analyzed by an RNAscope analysis using a probe against HLA-A*02:01. **b,** From the relapse biopsy, the normal epidermis with intact HLA-A*02:01 expression (bottom panel) and the tumor cells with a lack of HLA-A*02:01 expression (right panel) are shown. Scale bar, left panel in A and top left panel in B: 500 μm; right panel in A and top right and bottom panel in B: 50 μm.